Photobiomodulation guided healing in a sub-critical bone defect in calvarias of rats

Angela Maria Paiva Magri [1, 2]*, Kelly Rossetti Fernandes [1], Hueliton Wilian Kido [1], Gabriela Sodano Fernandes [1], Stephanie de Souza Fermino [1], Paulo Roberto Gabbai-Armelin [1], Franscisco José Correa Braga [3], Cintia Pereira de Góes [1], José Lucas dos Santos Prado [1], Renata Neves Granito [1], Ana Claudia Muniz Rennó [1]

1: Federal University of São Paulo (UNIFESP). Rua Silva Jardim, 136, Santos, SP, 11015020, Brazil.
2: University Center of the Guaxupé Educational Foundation (UNIFEG), Avenida Dona Floriana, 463, Guaxupé, MG, 37800000, Brazil.
3: Consulmat LTDA, Rua Juan Lopes, 159, São Carlos, SP, 13567-020, Brazil.

Background: Photobiomodulation presents stimulatory effects on tissue metabolism, constituting a promising strategy to produce bone tissue healing.
Objective: the aim of the present study was to investigate the in vivo performance of PBM using an experimental model of cranial bone defect in rats.
Material and Methods: rats were distributed in 2 different groups (control group and PBM group). After the surgical procedure to induce cranial bone defects, PBM treatment initiated using a 808 nm laser (100 mW, 30 J/cm^2, 3 times/week). After 2 and 6 weeks, animals were euthanized and the samples were retrieved for the histopathological, histomorphometric, picrosirius red staining and immunohistochemistry analysis.
Results: Histology analysis demonstrated that for PBM most of the bone defect was filled with newly formed bone (with a more mature aspect when compared to CG). Histomorphomeric analysis also demonstrated a higher amount of newly formed bone deposition in the irradiated animals, 2 weeks post-surgery. Furthermore, there was a more intense deposition of collagen for PBM, with ticker fibers. Results from Runx-2 immunohistochemistry demonstrated that a higher immunostaining for CG 2 week's post-surgery and no other difference was observed for Rank-L immunostaining.
Conclusion: This current study concluded that the use of PBM was effective in stimulating newly formed bone and collagen fiber deposition in the sub-critical bone defect, being a promising strategy for bone tissue engineering.

Key words: photobiomodulation • low-level laser therapy • bone healing • calvarial bone defect.

Introduction

The stimulatory effects of low-level laser therapy (LLLT) or more recently, photomobiomodulation (PBM) on biological tissues, have been highlighted for many studies [1-4], including the ability of modulating inflammatory processes after an injury, accelerating soft and hard tissue healing and stimulating neoangiogenesis [5-7]. The action of PBM can be explained mainly by the interaction of laser light and tissues, which generates a series of modifications in cell metabolism. When PBM is applied to tissue, light is absorbed by chromophore photoreceptors located in the cells, stimulating the mitochondrial respiration, the production of molecular oxygen and ATP synthesis [4, 8-10]. These effects can lead to increased expression of genes related to protein synthesis, cell migration and proliferation, anti-inflammatory signaling, anti-apoptotic proteins and antioxidant enzymes. Also, stem cells and progenitor

Addressee for Correspondence:
Angela Maria Paiva Magri
Department of Biosciences
Federal University of São Paulo (UNIFESP)
Rua Silva Jardim, 136, Santos, SP – Brazil.
Phone: +55 13 3229 0223
E-mail: angela.magri@yahoo.com.br

Received date: March 23rd, 2019
Accepted date: June 5th, 2019

cells appear to be particularly susceptible to PBM [10-12].

Based on these effects, this therapeutic intervention has been also used to stimulate bone metabolism and fracture consolidation [13-16]. Favaro-Pipi *et al.* [17] showed that 830nm laser (50 W/cm², 50 J/cm², 30 mW) produced an increase in the expression of genes related to bone differentiation, mainly BMP4, ALP and Runx-2 expression in an experimental model of bone defects in rats, demonstrating that this treatment is able of improving bone healing. Moreover, microarray analysis demonstrated that PBM produced an upregulation of genes related to the inflammatory process (MMD, PTGIR, PTGS2, PTGER2, IL1, 1IL6, IL8, IL18) and angiogenic activities (FGF14, FGF2, ANGPT2, ANGPT4 and PDGFD) in an experimental model of tibial bone defects in rats [1, 18].

Although all the positive effects of PBM have already been demonstrated, most of the studies are performed using non-critical bone defects, which is a limiting factor. In this context, it is highly required the use of sub-critical and critical models, which can better simulate clinical conditions of non-union fractures and pseudarthrosis. In view of the aforementioned, it was hypothesized that the treatment of sub-critical bone defects with PBM would be able of accelerating tissue metabolism, stimulating bone healing. Consequently, the present study aimed to evaluate the biological temporal modifications (using 2 experimental periods) of PBM on newly formed bone using a 5mm cranial bone defect trough histological, histomorphometry and immunohistochemistry analysis.

Materials and Methods

In vivo study

Third -two male Wister rats (12 weeks, 300-350g) were used as experimental animals. All animals were submitted to the surgical procedure to perform the critical cranial size bone defects. Animals were randomly divided into 2 groups (n=16 per group): Control Group (CG) and PBM Group (PBM). Each group was divided into two subgroups, euthanized by CO_2 suffocation after 2- and 6-weeks post-surgery (n = 8 for each subgroup). All animals were maintained under controlled temperature (22 ± 2°C), light–dark periods of 12 h and had free access to water and standard food. This study was approved by the Animal Care Committee guidelines of the Federal University of São Paulo (CEUA nº 9574290614).

Surgical procedures

For the surgical procedures, rats were submitted to anaesthesia with a combination of ketamine (80 mg/kg), xylazine (8 mg/kg), acepromazine (1 mg/kg) and fentanyl (0.05 mg/kg). To insert implants, the animals were immobilized, and the skull was shaved, washed and disinfected with povidone-iodine. Using aseptic techniques, an incision was made through the skin and the periosteum of the skull and a full-thickness flap was obtained. A 5 mm defect was created in the parietal region using a bone trephine drill (3i Implant Innovations Inc., Palm Beach Gardens, USA) under copious saline irrigation [19, 20]. The preset implants were placed in the created defect, according to a randomization scheme. Thereafter, the wound was closed with resorbable Vicryl® 5-0 (Johnson & Johnson, St.Stevens-Woluwe, Belgium) after which the skin was also sutured with nylon (Agraven®; InstruVet BV, Cuijk, The Netherlands). Four animals were housed per cage and the intake of water and food was monitored in the initial post-operative period. Further, rats were given appropriate postoperative care and animals were observed for signs of pain, infection and proper activity.

PBM treatment

The treatment with PBM started immediately after the surgery with a Photon Lase III equipment (DMC, São Carlos, Brazil). PMB parameters are described in **Table 1**. The irradiation was performed at one point, above and in the centre of the created defect, by the punctual contact technique. Three applications per week were performed, in non-consecutive days, totalling 6 and 18 sessions, respectively 2 and 6 weeks.

Histopathology

After the euthanasia, the skull parts were collected and fixed in 10% buffer formalin (Merck, Darmstadt, Germany) for 48 h, decalcified in 4% ethylenediaminetetraacetic acid (EDTA) (Merck, Darmstadt, Germany) and embedded in paraffin blocks. Thin sections (5 µm) were prepared using a microtome (Leica Microsystems SP 1600, Nussloch, Germany). Three sections of each specimen were stained with haematoxylin and eosin (Merck, Darmstadt, Germany) and examined using light microscopy

Table 1: PBM parameters

Parameters	
Wavelength	808 nm (infrared)
Laser frequency	Continuous output
Optical output	100 mW
Spot size	0.028 cm²
Power density	3.57 W/cm²
Dose	30 J/cm²
Energy	0.84 J
Time per point	8 s
Application mode	Stationary in skin contact mode

(Leica Microsystems AG, Wetzlar, Germany, Darmstadt-Germany) [2, 21, 22]. The presence of inflammatory process, granulation tissue, newly formed bone and material degradation were qualitatively evaluated in the laminas. The analysis was performed in a blinded way (AMPM).

Histomorphomeric analysis

Samples were quantitatively scored by using the semi-automatic image-analysing OsteoMeasure System (Osteometrics, Atlanta, GA, USA). All amount of newly formed bone in all samples were quantified separately for each specimen in order to compare between the experimental groups. For that, it was used the following parameter: osteoblast number per tissue area (N.Ob/T.Ar, /mm²), bone volume fraction (BV/TV, %), percentage of bone surface occupied by osteoblast (Ob.S/BS), and biomaterial volume per tissue area (BM.V/TV, %). In addition, the analysis was performed by two experienced observers (CPG and JLSP), in a blinded way.

Picrosirius red staining
Qualitative analysis

For the qualitative analysis, the samples were dewaxed and rehydrated, still immersed in 0.1% picrosirius red solution (Sirius red 0.1 g dissolved into 100 mL saturated picric acid solution) for 60 minutes of staining. After that, the samples were washed for 5 minutes, restrained with Harris haematoxylin (Merck) for 10 second. Following, the slides were dehydrated with gradient alcohol, and finally treating with xylene solvent and sealing with entellan (Sigma). The morphology, amount, and distribution of the collagen were observed under a polarized light microscope (AxioVision, Carl Zeiss, Jena, Germany). Type I collagen fibers, under a polarized light microscope, appear as yellow, orange-red, or red thick fibers.

Quantitative analysis

For quantitative analysis, photomicrographs from sections stained with Picrosirius-were taken by using a microscope (Axioshop 40 microscope, Carl Zeiss, Germany) under polarized (Sirius red staining) light, at 200x magnification [23]. This method allows to assess the presence, thickness and organization of the collagen fibers. For measurement, 3 images were taken for each specimen and using the "Imagen J software" (resolution of 1360 x 1024), the degree of gray scale of all images (1 to 255) were measured (with the higher values indicating an increased deposition of collagen). The values were expressed in percentage of the intensity of pixels (%) [24]. The analysis was performed in a blinded way (AMPM)

Immunohistochemistry analysis

For immunohistochemistry analysis, it was used the protocol described previously [2, 21], using the streptavidin–biotin-peroxidase method. Briefly, paraffin from the sections was removed with xylene. Then, the specimens were rehydrated in graded ethanol and pre-treated with 0.01 M citric acid buffer (pH 6) in a steamer for 5 min. To inactivate the endogenous peroxidase was used hydrogen peroxide in phosphate-buffered saline (PBS) for 5 min and blocked with 5% normal goat serum in PBS for 10 min. Following, the primary antibody was incubated with anti-Runx-2 polyclonal (code: sc-8566, Santa Cruz Biotechnology, USA) at a concentration of 1:300, and anti-Rank-L polyclonal (code: sc-7627, Santa Cruz Biotechnology, USA) also at a concentration of 1:300. The primary antibodies were incubated overnight at 4°C. Then, it was used the biotin-conjugated secondary antibody anti-rabbit IgG (Vector Laboratories, Burlingame, CA, USA) at a concentration of 1:200 in PBS for 1 h. Afterwards, samples were incubated with avidin biotin complex conjugated to peroxidase for 45 min. To reveal the immunostaining was used 0.05% solution of 3-3'-diaminobenzidine solution and restained with Harris haematoxylin (Merck) for 10 second. Finally, the specimens were analysed through the qualitatively (presence and location of the immunomarkers) and semi-quantitatively assess by using a light microscopy (Leica Microsystems AG, Wetzlar, Germany) according to a previously described scoring scale from 1 to 4 (1 = absent (0% of immunostaining), 2 = weak (1 – 35% of immunostaining), 3 = moderate (36 – 67% of immunostaining), and 4 = intense (68 – 100% of immunostaining) [2, 15]. The analysis was performed in a blinded way (AMPM).

Statistical analysis

Data were analysed and displayed in tables and graphs, and the values expressed as mean and standard deviation. In the statistical analysis, the distribution of variables was tested using the Shapiro-Wilk normality test. For the analysis of multiple comparisons, ANOVA was used with post hoc Tukey for parametric data and nonparametric data, the Kruskal-Wallis test was used with post hoc Dunn. The level of significance was set at 5 % ($p \leq 0.05$). All statistical analyses were performed using GraphPad Prism version 6.01.

Results

Histopathological analysis
Two weeks

Figure 1 shows a representative histological section of the experimental groups after 2 weeks post-surgery. In this experimental period, for CG, most of the defect was filled by granulation and conjunctive tissue, with some areas of newly formed bone at the borders of the defect **(Figure 1A and B)**. For PBM, granulation tissue was observed in most regions, with bone ingrowth being observed at the edges of the defect (surrounding the granu-

lation tissue). Also, some thick trabeculae from the borders to the centre region of the injury were presented **(Figure 1C and D)**.

Six weeks

An overview of the representative histological sections of all experimental groups after a 6 weeks implantation period can be observed in **Figure 2**. For CG, newly formed bone was seen in all extension of the defect. In addition, no granulation or conjunctive tissue was observed **(Figure 2A and B)**. Similar histological patterns were observed for PBM treated animals, however, the tissue mor-

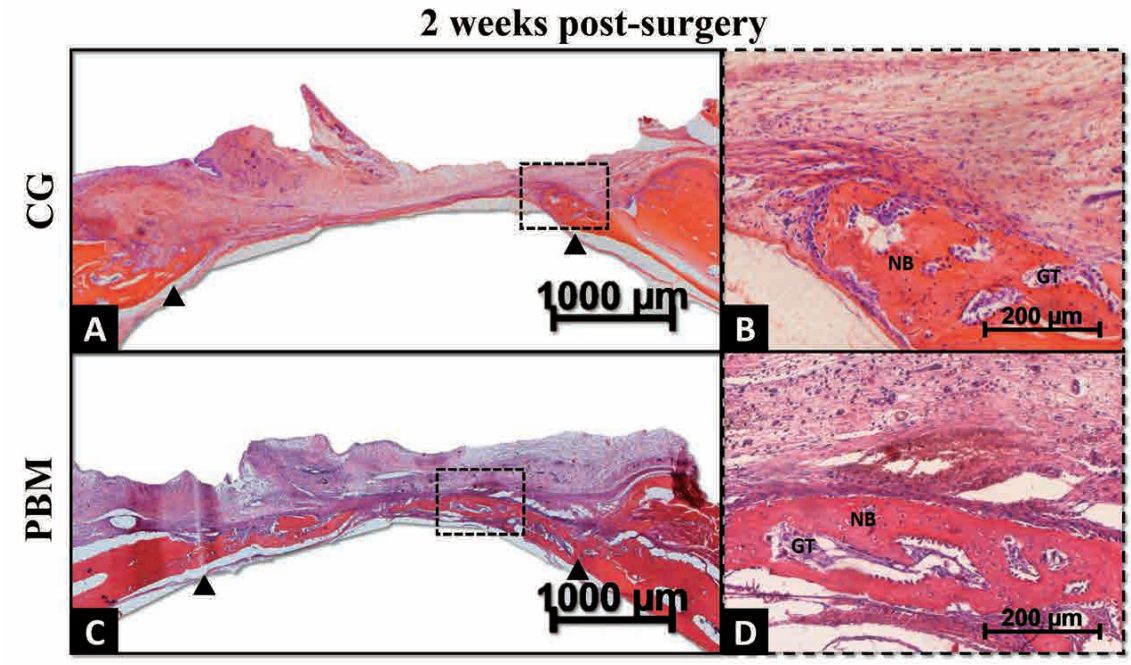

Figure 1: Representative histological sections of experimental groups. (A, B) CG; (C, D) PBM; after 2 weeks. NB - newly formed bone; RM – residual material. Hematoxylin and eosin. Scale bar = 1000 µm (mag. x2.5) and scale bar = 200 µm (mag. x20).

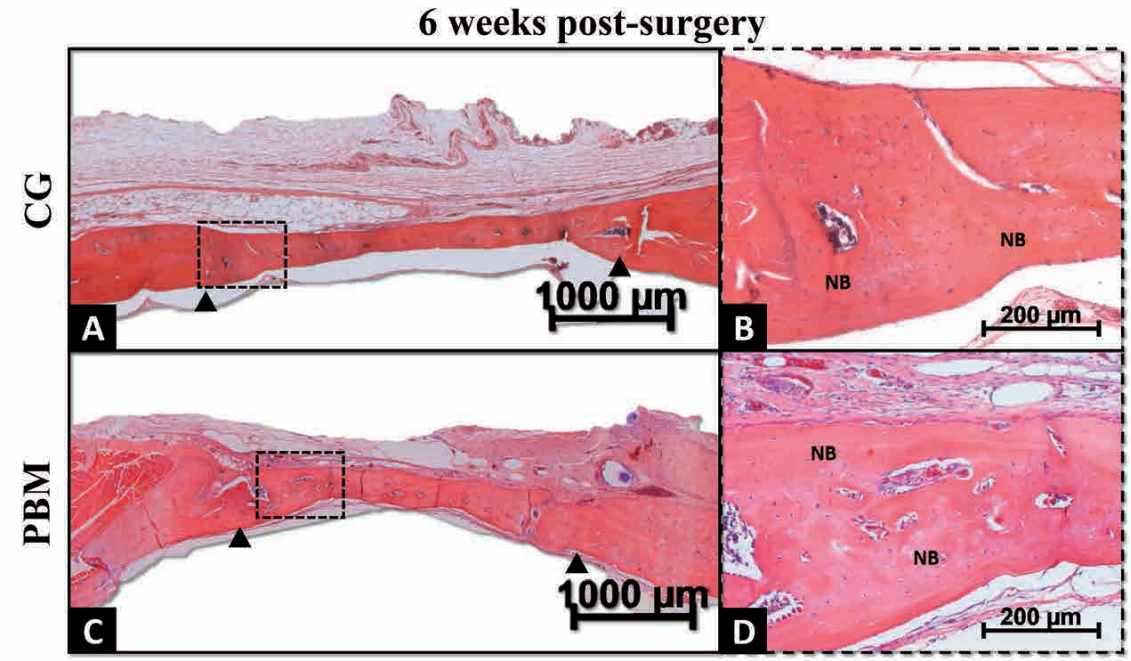

Figure 2: Representative histological sections of experimental groups. (A, B) CG; (C, D) PBM after 6 weeks. NB - newly formed bone; RM – residual material. Hematoxylin and eosin. Scale bar = 1000 µm (mag. x2.5) and scale bar = 200 µm (mag. x20).

phology seemed more mature, with thicker trabeculae compared to CG **(Figure 2C and D)**.

Histomorphometric analysis

Table 2 shows the variables of the histomorphometric analysis. At 2 weeks post-surgery, for PBM, it was evidenced a higher value of BV/TV (p = 0.0076) and N.Ob / T.Ar (p = 0.0004) in comparison to CG. In the second experimental period was no difference between the groups.

Picrosirius red staining analysis
Qualitative analysis

Figure 3 shows the photomicrographs of all experimental groups stained with picrosirius red, after 2 and 6 weeks of implantation. At 2 weeks post-surgery, CG and PBM, collagen fibers could be observed mainly at the borders of the bone defect **(3A and C)**. In the second experimental period, for CG, bone defect was filled with well interconnected collagen fibers **(Figure 3B)**. Similar findings were observed for PBM, which also presented connected fibers along the defect extension (thicker fibers compared to 2 weeks) **(Figure 3D)**.

Quantitative analysis

Figure 4 shows the quantification of the presence of collagen through of the intensity of pixels. It is possible to observe that no difference was observed comparing both groups, at 2- and 6-weeks post-surgery.

Table 2: Variables of the histomorphometric analysis 2- and 6-weeks post-surgery

Parameter	2 weeks		6 weeks	
	CG	PBM	CG	PBM
Ob.S/BS (%)				
Mean	31.0	37.2	14.2	20.5
SD	9.2	6.7	3.2	6.7
N.Ob/T.Ar				
Mean	133.8	334.0	140.1	107.8
SD	83.1	59.8	49.9	48.4
BV/TV (%)				
Mean	12.7	26.6*	52.5	28.2
SD	10.6	8.5**	9.1	16.1

SD = standard deviation. *PBM vs CG (2 weeks), p = 0.0076; **PBM vs CG (2 weeks), p = 0.0004. Mann Whitney test.

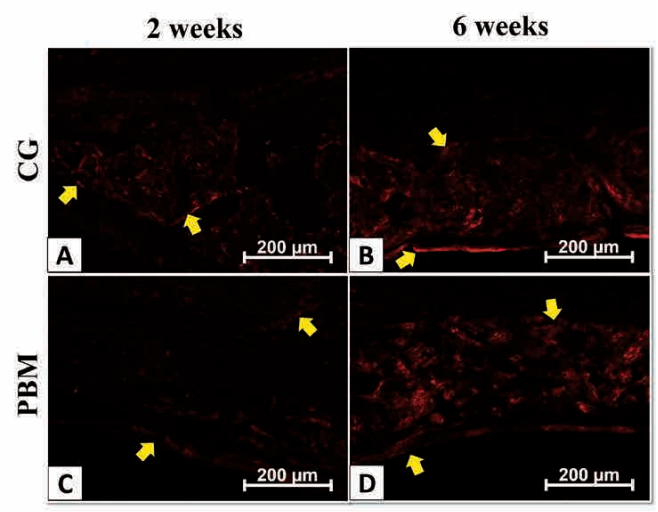

Figure 3: Micrographs of picrosirius red stained bone sections with polarized light. (A, B) CG; (C, D) PBM after 2- and 6-weeks post-surgery, respectively. Picrosirius red stain. Scale bar = 200 µm (mag. x20).

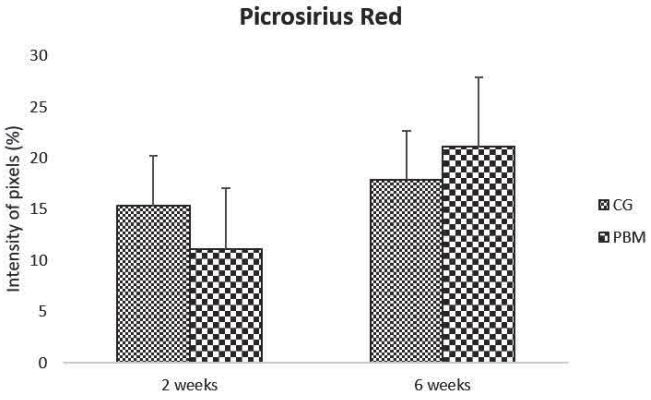

Figure 4: Means and standard deviation of intensity of pixels of picrosirius red. BG/PLGA vs BG/PLGA/PBM (p = 0.0188). Dunn's test.

Immunohistochemistry
Runx-2
Qualitative analysis

Positive Runx-2 immunostaining was observed in all experimental groups 2 weeks post-surgery **(Figure 5)**. For CG, Runx-2 immunostaining was observed mainly in the periosteum **(Figure 5A)**. Furthermore, for PBM, Runx-2 immunostaining was seen mainly in the conjunctive tissue and in the newly formed bone **(Figures 5C)**. At 6 weeks post-surgery, Runx-2 immunostaining was detected in few regions of the periosteum in CG and PBM (**Figure 5B and D**, respectively).

Semi-quantitative analysis

Figure 6 presented the semi-quantitative analysis of Runx-2 immunostaining. It is possible to observe a higher immunostaining for CG in comparison to PBM (p = 0.0069) at 2 weeks post-surgery. No difference was observed at 6 weeks post-surgery.

Rank-L
Qualitative analysis

Figure 7 demonstrates the qualitative analysis of Rank-L immunostaining. At 2 weeks post-surgery, all experimental groups presented positive Rank-L immunostaining mainly in the conjunctive tissue and in newly formed bone (Figure 7A and C).

At 6 weeks post-surgery, Rank-L immunostaining for CG and PBM was noticed mainly in the periosteum and conjunctive tissue **(Figure 7B and D)**.

Semi-quantitative analysis

Figure 8 demonstrates the semi-quantitative analysis for Rank-L immunostaining. It is possible to observe that no difference was observed comparing both groups, at 2- and 6-weeks post-surgery.

Discussion

In this study, the biological effects of PBM on bone healing in a sub-critical experimental model were evaluated. It was hypothesized that this therapy would be able of upregulating the immunostaining markers related to osteoblast differentiation, stimulating collagen and newly formed bone deposition. The main findings from the histological analysis showed that PBM treated animals presented a higher deposition of granulation tissue and newly formed bone in the area of the defect in both experimental periods. Also, the qualitative analysis of picrosirius staining demonstrated that the collagen fibers were ticker in the irradiated group. Runx-2 immunostaining presented higher values for CG 2 weeks post-surgery and no difference was observed for Rank-L immunostaining for both groups.

It is well known that PBM constitutes a promising effective therapeutic intervention able of stimulating bone tissue and producing healing [1, 2, 25]. In the present study, histological findings demonstrated that PBM was able of stimulating newly bone deposition at the region of the defect. Many authors demonstrated that PBM was able of stimulating mesenchymal cells and osteoblasts, culminat-

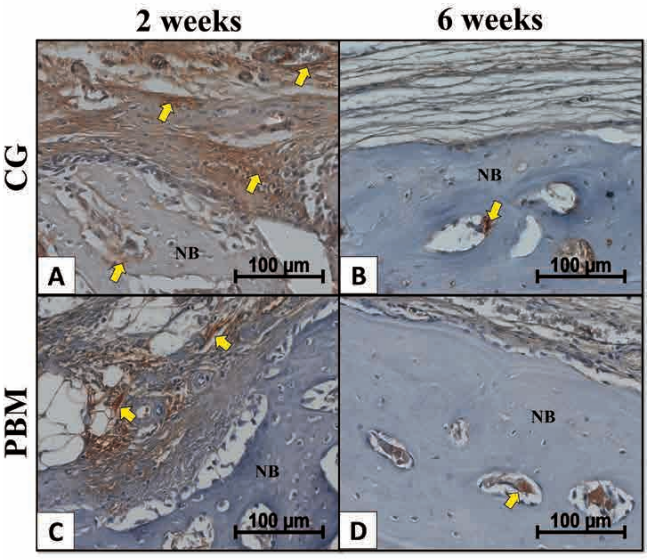

Figure 5: Immunohistochemistry of Runx-2. CG (A, B); PBM (C, D); after 2- and 6-weeks post-surgery, respectively. Arrow indicates Runx-2 immunostaining. Scale bar = 100 µm.

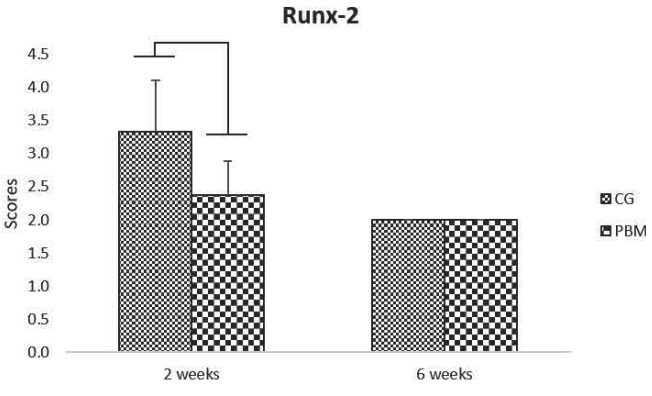

Figure 6: Means and standard deviation of scores immunohistochemistry of Runx-2. 2 weeks: CG vs PBM, p = 0.0069. T test.

ing in the increase of newly formed bone deposition [26-28]. Histomorphometry analysis corroborates the qualitative histological findings, presenting a higher value of BV/TV in the irradiated animals, 2 weeks post-surgery. The results of the present study may suggest that the energy from PBM was adequate to stimulate properly bone cells and consequently, increase the amount of newly formed bone. Shakouri *et al.* [29] showed that PBM enhanced the callus development in the early stage of the healing process in rabbits, with improvement in the biomechanical properties of bone healing. Also, PBM has been demonstrating to stimulate fracture bone healing in osteoporotic rats [30]. Furthermore, it has been reported that PBM has a stimulatory effect on neovascularization by stimulating the secretion of angiogenic factors, which together with the osteogenic properties of PBM might further influence bone formation in the irradiated animals [31].

Moreover, both CG and PBM presented deposition of collagen fibers in the region of the defect, with thicker fibers being observed in the irradiated group, resembling a more mature tissue after 6 weeks post-surgery. It is known that collagen is the most found protein in the human body and the major component of organic matrix of bone tissue [32, 33]. During the process of fracture healing, an intense deposition of collagen matrix deposition is observed, which is, progressively, enriched with mineralized tissue [34]. For the present study, the thicker collagen fibers in the PBM treated animals, may indicate that the PBM possibly was able of anticipating cell recruitment and consequently, introducing earlier the normal phases of healing and the deposition of organic matrix, which may result in a mineralization and remodeling in the area of the defect [34, 35]. These results are in agreement those of [24] who also found a higher deposition of collagen fibers after PBM in a model of tibial bone defect in tibia of rats.

Additionally, Runx-2 is essential for the recruitment of mesenchymal cells to the osteoblast lineage and differentiation and maturation of osteoblasts [36, 37]. Runx-2 influences the function of osteoblasts by regulating the expression of many osteoblast-related genes as ALP, OC, osteopontin and collagen type I [36, 37]. The results of Runx-2 immunostaining from the present study demonstrated that CG presented higher values 2 weeks post-surgery. These findings may be explained by the set point analyzed after the surgical procedure (15 days). As it is known that PBM induces an earlier recruitment of stem cells and pre-osteoblastic cells [38], it is possible to suggest that the peak of Runx-2 synthesis may happen before 2 weeks in the irradiated group (in a period when the osteoblasts were more active). This hypothesis may be confirmed by the higher amount of newly formed bone in the defect area in the PBM group, indicating a higher activity of osteoblasts and consequently, a higher presence of Runx-2. This statement supports the idea that PBM shows an osteogenic potential. Interestingly, in the second experimental period, no difference was observed.

Similarly, Rank-L is regulator factor for osteoclast cell activation and it is involved with endochondral resorption and bone remodeling [39, 40]. Interestingly, no difference in Rank-L immunostaining was observed between groups in both experimental periods. This fact suggests that PBM did not influence the amount of macrophages/

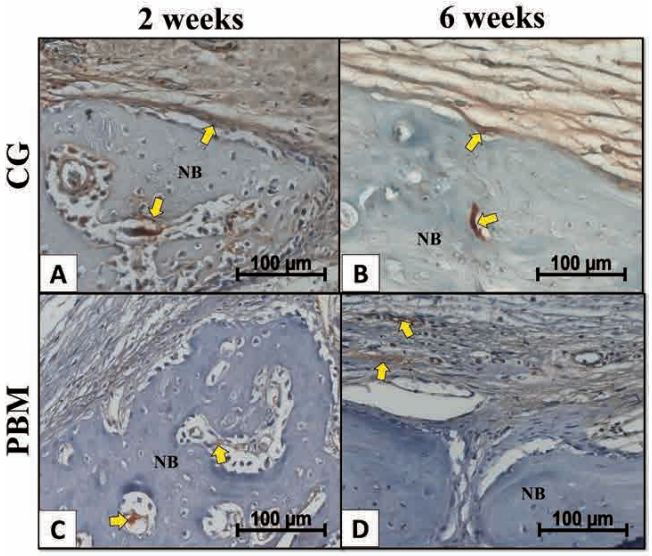

Figure 7: Immunohistochemistry of Rank-L. CG (A, B); PBM (C, D); after 2- and 6-weeks post-surgery, respectively. Arrow indicates Runx-2 immunostaining. Scale bar = 100 µm.

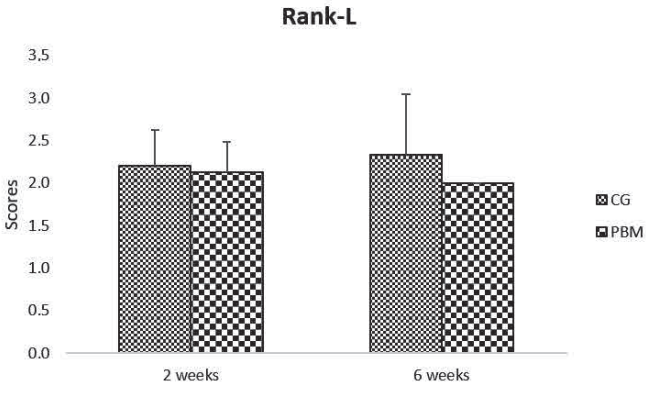

Figure 8: Means and standard deviation of scores immunohistochemistry of Rank-L T test.

osteoclasts bone tissue in the area of the defect and may imply that PBM stimulatory effects is related more to the stimulation of osteoblast acitivity. The findings of the present study corroborate those of Tim *et al*. [15] who found no statistically significant difference in Rank-L immunostaining between CG and PMB 15, 30- and 45-days post-surgery in a model of tibial bone defect in rats. Patrocinio-Silva *et al*. [41] also did not find any difference in Rank-L immunostaing after PBM in a model of tibial bone defect in diabetic rats.

In summary, this study revealed that PBM was able of stimulating newly formed bone and collagen fiber deposition, which indicate that this therapeutical intervention constitutes a promising treatment for bone tissue repair. Further long-term studies should be carried out to provide additional information concerning the application of PBM, especially in critical bone defects and compromised situations such osteoporosis.

Conclusion

The results of the present study support the notion that that PBM improved the process of bone repair in a sub-critical bone defect as a result of stimulation of the newly formed bone and increase of collagen fibers deposition. More studies should be developed to investigate the optimal parameters of PBM using critical models.

References

1: Tim CR, Bossini PS, Kido HW, et al. Effects of low-level laser therapy on the expression of osteogenic genes during the initial stages of bone healing in rats: a microarray analysis. *Lasers in medical science*. 2015;30(9):2325-2333.

2: Magri AM, Fernandes KR, Assis L, et al. Photobiomodulation and bone healing in diabetic rats: evaluation of bone response using a tibial defect experimental model. *Lasers in medical science*. 2015;30(7):1949-1957.

3: Duarte KCN, Soares TT, Magri AMP, et al. Low-level laser therapy modulates demyelination in mice. *Journal of photochemistry and photobiology B, Biology*. 2018;189:55-65.

4: Hamblin MR. Mechanisms and applications of the anti-inflammatory effects of photobiomodulation. *AIMS biophysics*. 2017;4(3):337-361.

5: Ruh AC, Frigo L, Cavalcanti M, et al. Laser photobiomodulation in pressure ulcer healing of human diabetic patients: gene expression analysis of inflammatory biochemical markers. *Lasers in medical science*. 2018;33(1):165-171.

6: de Lima FM, Bjordal JM, Albertini R, Santos FV, Aimbire F. Low-level laser therapy (LLLT) attenuates RhoA mRNA expression in the rat bronchi smooth muscle exposed to tumor necrosis factor-alpha. *Lasers in medical science*. 2010;25(5):661-668.

7: Hegedus B, Viharos L, Gervain M, Galfi M. The effect of low-level laser in knee osteoarthritis: a double-blind, randomized, placebo-controlled trial. *Photomedicine and laser surgery*. 2009;27(4):577-584.

8: Karu T. High-tech helps to estimate cellular mechanisms of low power laser therapy. *Lasers in surgery and medicine*. 2004;34(4):298-299.

9: Huang YY, Chen AC, Carroll JD, Hamblin MR. Biphasic dose response in low level light therapy. *Dose-response: a publication of International Hormesis Society*. 2009;7(4):358-383.

10: Huang YY, Sharma SK, Carroll J, Hamblin MR. Biphasic dose response in low level light therapy - an update. *Dose-response: a publication of International Hormesis Society*. 2011;9(4):602-618.

11: Karu TI, Pyatibrat LV, Afanasyeva NI. Cellular effects of low power laser therapy can be mediated by nitric oxide. *Lasers in surgery and medicine*. 2005;36(4):307-314.

12: de Freitas LF, Hamblin MR. Proposed Mechanisms of Photobiomodulation or Low-Level Light Therapy. *IEEE journal of selected topics in quantum electronics: a publication of the IEEE Lasers and Electro-optics Society*. 2016;22(3).

13: Freitas NR, Guerrini LB, Esper LA, et al. Evaluation of photobiomodulation therapy associated with guided bone regeneration in critical size defects. In vivo study. *Journal of applied oral science : revista FOB*. 2018;26:e20170244.

14: Fernandes KR, Ribeiro DA, Rodrigues NC, et al. Effects of low-level laser therapy on the expression of osteogenic genes related in the initial stages of bone defects in rats. *Journal of biomedical optics*. 2013;18(3):038002.

15: Tim CR, Pinto KN, Rossi BR, et al. Low-level laser therapy enhances the expression of osteogenic factors during bone repair in rats. *Lasers in medical science*. 2014;29(1):147-156.

16: Renno AC, McDonnell PA, Crovace MC, Zanotto ED, Laakso L. Effect of 830 nm laser phototherapy on osteoblasts grown in vitro on Biosilicate scaffolds. *Photomedicine and laser surgery*. 2010;28(1):131-133.

17: Favaro-Pipi E, Ribeiro DA, Ribeiro JU, et al. Low-level laser therapy induces differential expression of osteogenic genes during bone repair in rats. *Photomedicine and laser surgery*. 2011;29(5):311-317.

18: Tim CR, Bossini PS, Kido HW, et al. Effects of low level laser therapy on inflammatory and angiogenic gene expression during the process of bone healing: A microarray analysis. *Journal of photochemistry and photobiology B, Biology*. 2016;154:8-15.

19: Luvizuto ER, Queiroz TP, Margonar R, et al. Osteoconductive properties of beta-tricalcium phosphate matrix, polylactic and polyglycolic acid gel, and calcium phosphate cement in bone defects. *The Journal of craniofacial surgery*. 2012;23(5):e430-433.

20: Kubota T, Hasuike A, Ozawa Y, et al. Regenerative capacity of augmented bone in rat calvarial guided bone augmentation model. *Journal of periodontal & implant science*. 2017;47(2):77-85.

21: Magri AMP, Fernandes KR, Ueno FR, et al. Osteoconductive properties of two different bioactive glass forms (powder and fiber) combined with collagen. *Applied Surface Science*. 2017;423:557-565.

22: Fernandes KR, Magri AMP, Kido HW, et al. Biosilicate/PLGA osteogenic effects modulated by laser therapy: In vitro and in vivo studies. *Journal of photochemistry and photobiology B, Biology*. 2017;173:258-265.

23: Biguetti CC, Cavalla F, Tim CR, et al. Bioactive glass-ceramic

bone repair associated or not with autogenous bone: a study of organic bone matrix organization in a rabbit critical-sized calvarial model. *Clinical oral investigations*. 2018.
24: Bossini PS, Renno AC, Ribeiro DA, et al. Biosilicate(R) and low-level laser therapy improve bone repair in osteoporotic rats. *Journal of tissue engineering and regenerative medicine*. 2011;5(3):229-237.
25: Sarvestani FK, Dehno NS, Nazhvani SD, et al. Effect of low-level laser therapy on fracture healing in rabbits. *Laser therapy*. 2017;26(3):189-193.
26: Santinoni CD, Oliveira HF, Batista VE, Lemos CA, Verri FR. Influence of low-level laser therapy on the healing of human bone maxillofacial defects: A systematic review. *Journal of photochemistry and photobiology B, Biology*. 2017; 169:83-89.
27: Noba C, Mello-Moura ACV, Gimenez T, Tedesco TK, Moura-Netto C. Laser for bone healing after oral surgery: systematic review. *Lasers in medical science*. 2018;33(3):667-674.
28: Skondra FG, Koletsi D, Eliades T, Farmakis ETR. The Effect of Low-Level Laser Therapy on Bone Healing After Rapid Maxillary Expansion: A Systematic Review. *Photomedicine and laser surgery*. 2018;36(2):61-71.
29: Shakouri K, Eftekharsadat B, Oskuie MR, et al. Effect of low-intensity pulsed ultrasound on fracture callus mineral density and flexural strength in rabbit tibial fresh fracture. *Journal of orthopaedic science : official journal of the Japanese Orthopaedic Association*. 2010;15(2):240-244.
30: Diniz JS, Nicolau RA, de Melo Ocarino N, do Carmo Magalhaes F, de Oliveira Pereira RD, Serakides R. Effect of low-power gallium-aluminum-arsenium laser therapy (830 nm) in combination with bisphosphonate treatment on osteopenic bone structure: an experimental animal study. *Lasers in medical science*. 2009;24(3):347-352.
31: Fortuna T, Gonzalez AC, Sa MF, Andrade ZA, Reis SRA, Medrado A. Effect of 670 nm laser photobiomodulation on vascular density and fibroplasia in late stages of tissue repair. *International wound journal*. 2018;15(2):274-282.
32: O'Brien FJ. Biomaterials & scaffolds for tissue engineering. *Materials Today*. 2011;14(3):88-95.
33: Oh JH, Kim HJ, Kim TI, Woo KM. Comparative evaluation of the biological properties of fibrin for bone regeneration. *BMB reports*. 2014;47(2):110-114.
34: Marsell R, Einhorn TA. The biology of fracture healing. *Injury*. 2011;42(6):551-555.
35: Rizwan M, Hamdi M, Basirun WJ. Bioglass(R) 45S5-based composites for bone tissue engineering and functional applications. *Journal of biomedical materials research Part A*. 2017;105(11):3197-3223.
36: Wallner O, Stark A, Muren O, Eisler T, Skoldenberg O. Unstable hip arthroplasties. A prospective cohort study on seventy dislocating hips followed up for four years. *International orthopaedics*. 2015;39(6):1037-1044.
37: Zhang Y, Xie RL, Croce CM, et al. A program of microRNAs controls osteogenic lineage progression by targeting transcription factor Runx2. *Proceedings of the National Academy of Sciences of the United States of America*. 2011;108(24): 9863-9868.
38: Ginani F, Soares DM, Barreto MP, Barboza CA. Effect of low-level laser therapy on mesenchymal stem cell proliferation: a systematic review. *Lasers in medical science*. 2015;30(8):2189-2194.
39: Hienz SA, Paliwal S, Ivanovski S. Mechanisms of Bone Resorption in Periodontitis. *Journal of immunology research*. 2015;2015:615486.
40: de Vernejoul MC. Sclerosing bone disorders. *Best practice & research Clinical rheumatology*. 2008;22(1):71-83.
41: Patrocinio-Silva TL, de Souza AM, Goulart RL, et al. The effects of low-level laser irradiation on bone tissue in diabetic rats. *Lasers in medical science*. 2014;29(4):1357-1364.

Conflict of interest
The authors declare no competing interests.

Acknowledgments
The authors would like to acknowledge funding agencies FAPESP (grant number: 2014/20546-0) and CNPq for the financial support of this research and CAPES for scholarship to AMPM. In addition, the authors would like to thank Dr. Ingrid Regina Avanzi for helping during some euthanasia of the animals and Prof. Dr. Flavia de Oliveira and Hananiah Tardivo Quintana for assistance with picrosirius analysis.